Multi-Disciplinary Optimization of Airship Envelope Shape

T.S.Kanikdale*

Department of Aerospace Engineering, Indian Institute of Technology Bombay, India

A.G.Marathe † and R.S.Pant ‡

Department of Aerospace Engineering, Indian Institute of Technology Bombay, India

This work aims at the arriving at the optimum shape of an airship envelope of fixed volume from aerodynamic and structural considerations, using the concept of multi-disciplinary design optimization. The multi-disciplinary nature of the problem is discussed and the corresponding objective functions and the constraints are elucidated. The strategies adopted are described along with the shape generation algorithm. *Fluent* CFD code has been used for computational experimentation in conjunction with SIMANN, simulated annealing code for optimization. The low fidelity model available in the literature was found to give large deviations from the physical value of envelope drag. The mathematical model for envelope drag estimation has been developed based on the detail study of results obtained through CFD experimentation. It was observed that the shape optimized for minimum drag shows a significant improvement over a reference GNVR shape. The multi-disciplinary nature of the problem is addressed by devising a composite objective function and corresponding results are presented.

Nomenclature

a	Major radius of ellipse (A-B) in figure2
b	Minor radius of ellipse (A-B) in figure2
C_D	Coefficient of drag
C_{DV}	Volumetric coefficient of drag
C_p	Coefficient of pressure
d	Maximum diameter of envelope
g	Acceleration due to gravity
l	Length of envelope
N	Number of grid points
R	Radius of leading spherical envelope cap
R_1	Major Radius of second ellipse (B-C) in figure 2
R_2	Minor Radius of second ellipse (B-C) in figure 2
R_e	Reynold's number
S	Total surface area

*Graduate student email: tushark@aero.iitb.ac.in

†Professor, email: anil@aero.iitb.ac.in

‡Associate Professor, email: rkpant@aero.iitb.ac.in

t	Thickness of airship membrane
V	Free stream velocity
x_1	X-coordinate of the start point of spline-I
x_2	X-coordinate of the start point of spline-II
x_3	X-coordinate of the end point of spline-II
X_{ymax}	X-coordinate of the position of maximum diameter (x_2)
y_1	Y-coordinate of the start point of spline-I
y_2	Y-coordinate of the start point of spline-II
y_3	Y-coordinate of the end point of spline-II
Symbols	
ρ_a	Density of air
ρ_{he}	Density of helium
σ_{max}	Maximum hoop stress per unit thickness
Acronym	
$DACE$	Design and Analysis of Computer Experiments
$SPACE$	Stochastic Process Analysis for Computer Experiments

I. Introduction

An airship is a lighter than air vehicle which obtains its lift due to buoyancy. The envelope, which generates lift, is the most important component of an airship. The envelope volume is determined from the required payload and maximum operating altitude, whereas the shape is usually decided from aerodynamic considerations, i.e. minimum drag. The aerodynamic considerations are reflected through minimum volumetric drag coefficient, whereas the structural considerations are brought in through minimum surface area and hoop stress, both of which directly result in lowest envelope weight.

II. Multi-Disciplinary Aspects

The three disciplines that directly influence airship envelope design with their own constraints and requirements are aerodynamics,structures and weight and balance. The aerodynamics of airship has been studied by many authors and based on experimental observations empirical relation for C_D has been proposed. It is shown that coefficient of drag C_D for axisymmetric streamline bodies is a function of thickness ratio ($d\,/\,l$).[1] Using the empirical correlations given by Khoury and Gillet[2] it is observed that, for the bodies with $(d/l) < 0.23$, an increase in maximum diameter reduces the total drag, but induces higher hoop stress . This illustrates one of the possible interactions among various disciplines which have to be handled during the optimization process.

A. Problem Formulation

The specific problem aims at developing a general tool to optimize the envelope shape for the individual objective functions or their weighted combinations as per the design requirements. Equality constraints of fixed volume ($1000\,m^3$) and fixed length ($26.7\,m$) are imposed. The constraint on envelope volume represents the fixed payload and fixed length constraint has arisen due to the stability requirement where the envelope length has strong influence over the control surface area. The drag, weight and maximum stress induced in the membrane are considered as three possible objective functions for the design of the airship envelope. The characteristics of optimal envelope shapes obtained are compared with a reference envelope shape (GNVR) whose aerodynamic characteristics are known. The details of this shape are shown in figure 1. Past studies[3] indicated that this shape corresponds to least volumetric coefficient of drag C_{DV} uunder the given operating conditions. One of the aims of this work is to confirm this and to obtain a better shape if possible.

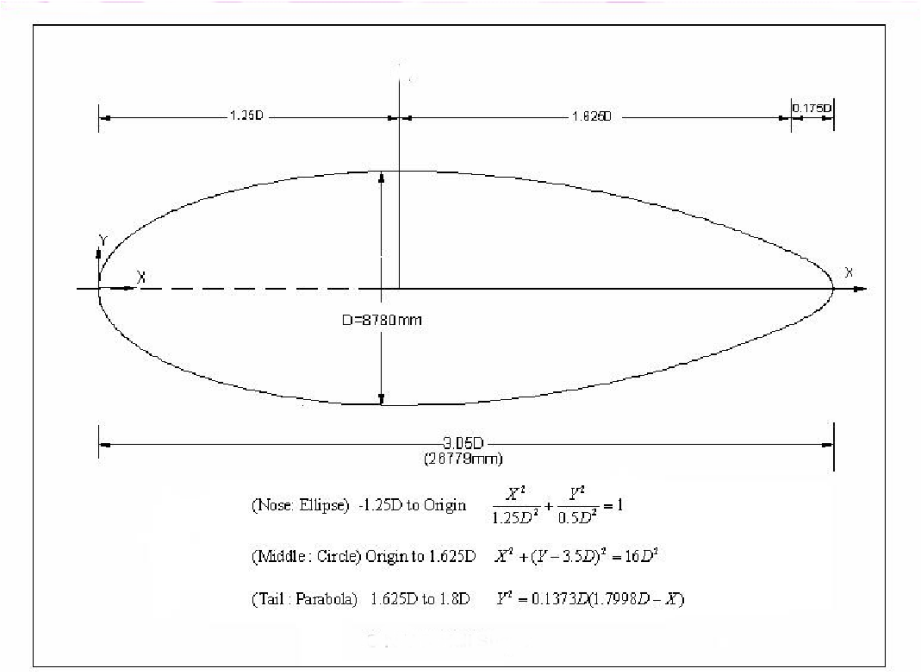

Figure 1. GNVR Envelope Shape

B. Strategy

The basic strategy to attempt the problem was to use the optimizer along with the "shape generation routine" which generates a shape and calculates the corresponding objective function for the specified design vector. High fidelity tools like Computational Fluid Dynamics code and Finite Element Method are the primary candidates to evaluate the objective functions like drag and stress respectively. The use of such high fidelity models render the optimization process highly time intensive.

Since the shape comprised of ellipses has proved to be aerodynamically efficient,[2] initially the geometry consisting of elliptical shapes and a parabola as shown in figure 2 is analyzed in axisymmetric and is being parametrized using two design variables (R_1, X_e). The complete envelope body and corresponding parameters are obtained by revolving the 2-D shape by 360^0 about X-axis. The requirements of fixed volume and length are implicitly taken care in the shape generation algorithm and it is noticed that for such geometry the maximum diameter comes out to be same as that of GNVR shape for any value of design vector specified .

III. Validation of *Fluent* using GNVR Data

Fluent 6.1 is selected as flow analysis tool which is a commercial state of art CFD software and is a well accepted industry standard package. The package offers flow and heat transfer modeling software suited to a wide range of applications. The same package is complemented by a another grid generation package *Gambit*. Many researchers have used the *Fluent* package to validate for the given application. Just to mention Z. Pateka and L. Smrcek[4] have validated *Fluent* code for determining aerodynamic characteristics of aircraft surfaces. Rachid Younsi *et.al*[5] have also validated *Fluent* code using the experimental data for the flow over

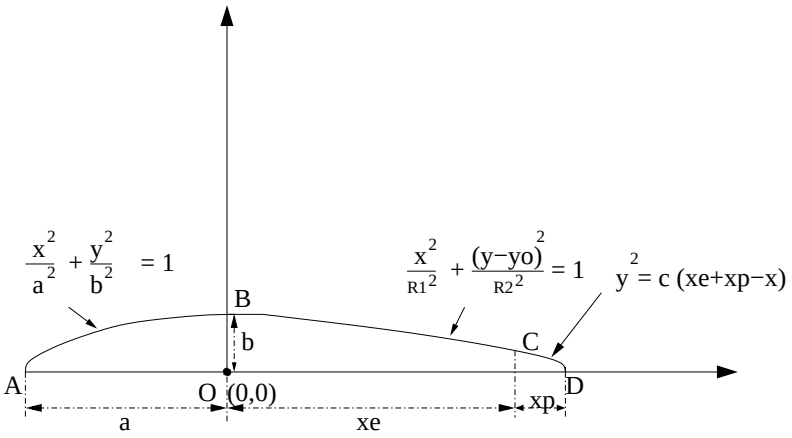

Figure 2. Generalized Shape Configuration using Basic Shapes

NACA 4415 airfoil as a cross-section of wind turbine blade.

To analyze the flow field, an axisymmetric structured grid was built around the upper half of the GNVR body in the semicircular computational domain using the commercial package *Gambit* as shown in figure 3.

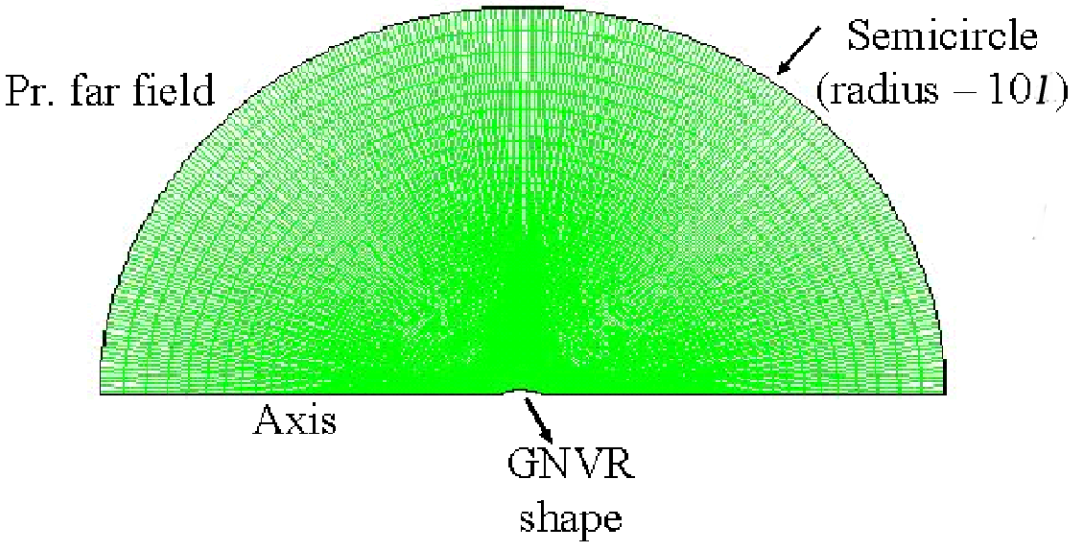

Figure 3. Structured Grid around GNVR body in Semicircular Domain

The flow boundary conditions are specified with zero angle of attack as

Mach Number = 0.15
Static Pr.= 0.875 bar

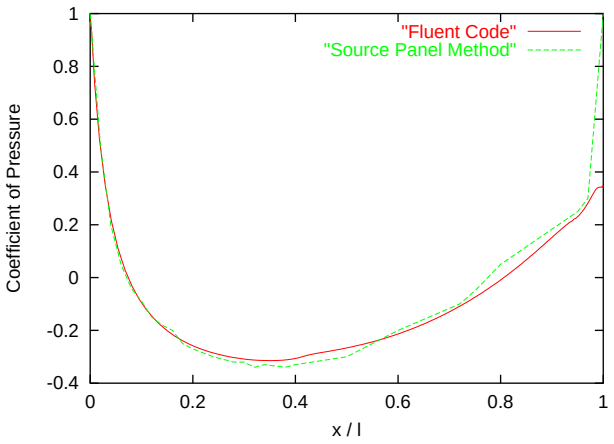

Figure 4. Comparison using C_p Distribution

Static temp.= 280.3 K

Fluent code required around 2.5 hrs to reach to steady state solution on a standard Pentium-III(650Hz) machine. The coefficient of pressure (C_p) distribution over the envelope surface is compared with reference values for GNVR shape calculated using source panel method by Narayana and Srilatha[3] and is shown in figure 4. The values closely match except near the trailing edge because of the flow seperation. The influence of computational domain size has also been studied and it is found that the solution obtained with semicircular computational domain with $10l$ radius exactly matches with that of $5l$ computational domain size.

Since the thrust required for the airship is dictated directly by the envelope drag ,it is preferable to take drag as a objective function in lieu of C_D . Hence the coefficient of drag based on volumetric area (C_{DV}) which gives direct indication of drag, is adopted as one of the objective functions. This volumetric coefficient of drag (C_{DV}) can be converted to coefficient of drag based on surface area using the transformation

$$C_D = \frac{C_{DV} * (Volume)^{2/3}}{S} \tag{1}$$

IV. Response Surface for C_{DV} using DACE

Since the design vector size was small for the configuration with primary shapes, it became economical to use the surrogate model technique like Design and Analysis of Computer Experiments (DACE) which resulted in response surface for C_{DV} . The design space is descretized using Orthogonal Latin Square method and the actual values for C_{DV} corresponding to the design points are calculated using *Fluent* code. The ranges for design variables are selected such that the entire design space lies in feasible region. figure 5 shows the response surface obtained for C_{DV} and its various views.

DACE requires the value of C_{DV} for sufficient number of airship bodies with varying envelope shapes. Though the shapes are geometrically different, they are more or less similar with small perturbation. Hence once the steady state solution for the reference body is achieved, it can be taken as initial guess for the another body for which solution is required. This technique is termed as slapping technique and is used for the current problem. It is observed that the time required for steady state solution for the same grid and boundary conditions reduced by nearly 40% of computational time per geometry. The resulted optimized shape for minimum C_{DV} found to be closely matching with GNVR shape and is shown in figure 6

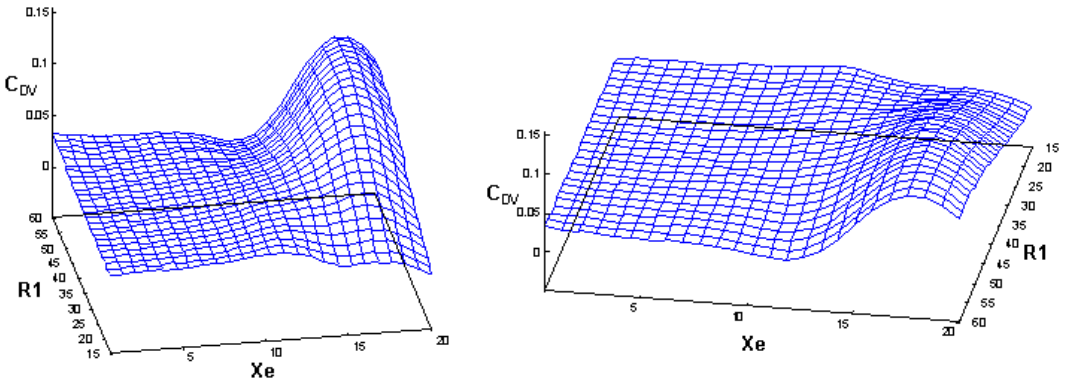

Figure 5. Response Surface for C_{DV} using DACE

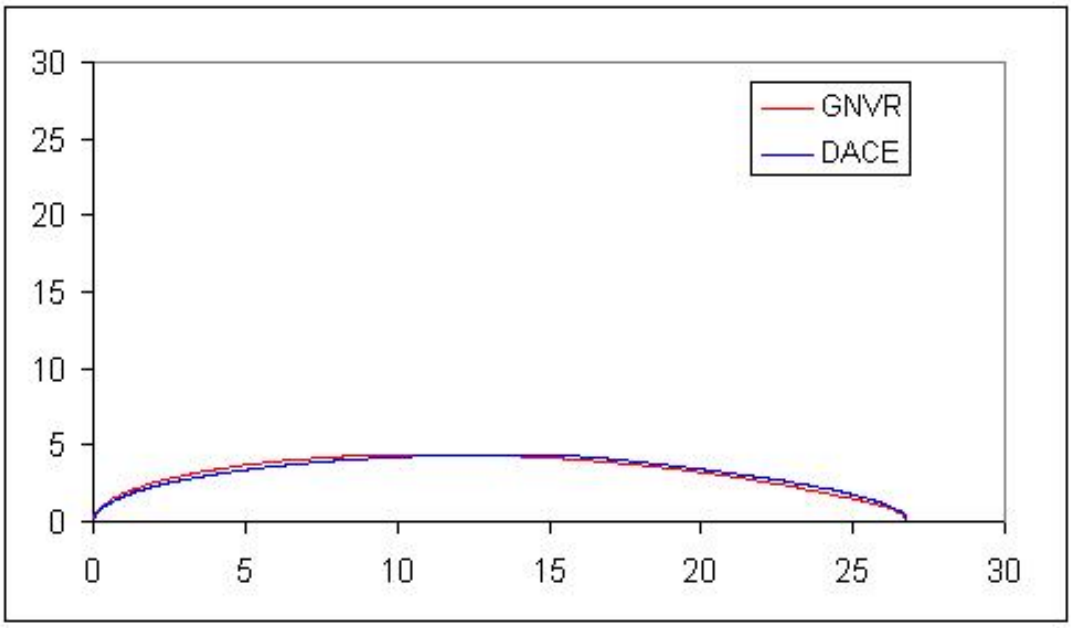

Figure 6. Optimized Shape (DACE) Vs GNVR Shape

V. Improved Shape Generation Algorithm

To explore the possibility of better shapes in view of the multi disciplinary aspect of optimization, the generalized configuration was improved to increase design space. The improved configuration comprised of two cubic splines with a spherical portion and parabola at the leading and trailing edge respectively as shown in figure 7. The governing equations for the geometric elements of the shape are listed below with reference to the origin at the leading edge of the envelope.

- Sphere (Circle in 2-D)

$$y^2 = 2xR - x^2 \tag{2}$$

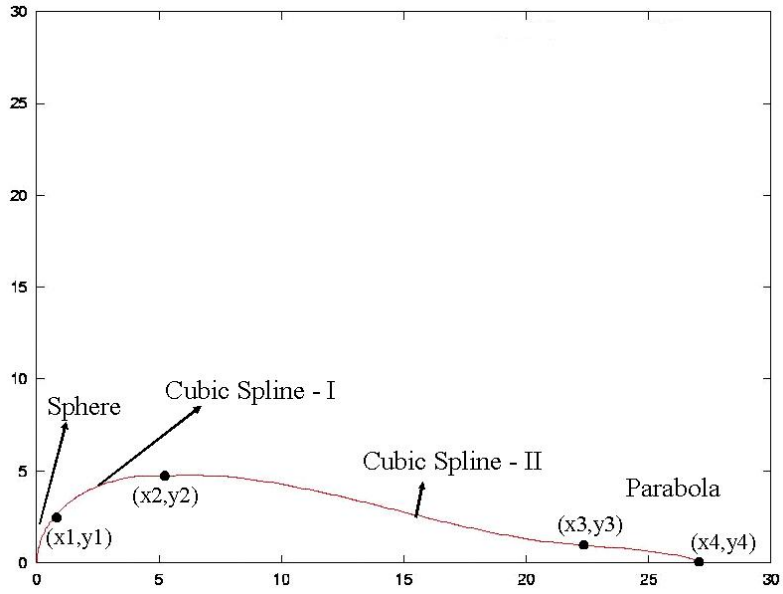

Figure 7. Improved Methodology for Envelope Shape Generation

- Spline I

$$y = a_1 x^3 + b_1 x^2 + c_1 x + d_1 \tag{3}$$

- Spline II

$$y = a_2 x^3 + b_2 x^2 + c_2 x + d_2 \tag{4}$$

- Parabola

$$y^2 = a_n (l - x) \tag{5}$$

A. Design Vector

The total number of unknowns as seen from the equations are eleven , namely (R,a_1,b_1,c_1,d_1,a_2,b_2,c_2,d_2,a_n,l). The size of the design vector can be found out after specifying constraints in the form of boundary conditions for the governing equations. The various constraints and conditions imposed on the geometry are as follows

1. Volume of airship = 1000 m^3
2. Slope continuity at point (x_1,y_1)
3. Slope continuity at point (x_2,y_2)
4. Slope continuity at point (x_3,y_3)
5. Slope at point (x_2,y_2) = 0

The length is deliberately kept in the design vector to investigate the effect of relaxing the length constraint. The size of the design vector must be 6 to find out 11 unknowns for 5 given conditions. The design vector for the concerned problem is chosen as

$$X_D = (x_1,\ x_2,\ y_2,\ x_3,\ y_3,\ l)$$

The set of linear equations were solved using Gauss-Jordan technique and the non linear equation for volume was coupled using the technique of successive approximation. Convex envelope shapes were discarded by forcing negative radius of curvature , since the shapes with convexcity particularly at the trailing portion would suffer from heavy pressure drag and such shapes were considered to have greater penalty in terms of manufacturing. Moreover the low fidelity empirical formulae for C_{DV} was applicable for streamline bodies only.

VI. Evaluation of Objective Functions

The optimization process using high fidelity models becomes highly time intensive. In the present approach, low fidelity models suggested in the literature have been incorporated in the optimizer instead of directly using high fidelity analysis to evaluate the objective functions.

A. Model Description

1. *Volumetric Coefficient of Drag (C_{DV})*

Khoury and Gillett[2] have given the formula for C_{DV} as a function of thickness ratio (d/l) for the streamline bodies of revolution. The coefficient of drag is calculated based on volumetric area $(Volume)^{2/3}$ at zero angle of attack and is depicted in Eq.6

$$C_{DV} = \frac{0.172(l/d)^{1/3} + 0.252(d/l)^{1.2} + 1.032(d/l)^{2.7}}{R_e^{1/6}} \tag{6}$$

The total drag on airship also depends upon cross-flow. Jones *et.al.*[6] have reported the correlation for drag in terms of axial and cross-flow drag coefficients. The effect of cross-flow, however is neglected in the present work.

2. *Total Surface Area (S)*

Total surface area has been considered as one of the objective functions as it gives the direct indication of the envelope weight. Total surface area for the envelope shape is estimated analytically as the equations governing the shape are known.

3. *Maximum Hoop Stress per Unit Thickness (σ_{max})*

Pant and gawale[7] have provided a procedure for estimation of total internal pressure. The maximum hoop stress per unit thickness is given by Eq. 7 and is depends mainly upon differential aerodynamic and internal pressure with respect to the ambient pressure and variation in hydrostatic pressure as depicted in Eq.8 The aerodynamic pressure arises due to the motion of the body. The internal pressure inside the envelope is generally taken 15% more than the dynamic pressure to ensure that the shape of the envelope is maintained during forward motion. The value for coefficient of pressure (C_p) required for $(\Delta P)_{aerodynamic}$ calculation is generally taken as 0.33 as suggested by Khoury and Gillett.[2] The differential aerodynamic and internal pressure are calculated using Eq.9 and Eq.10 respectively.

$$\sigma_{max} = \frac{\Delta P d}{2} \tag{7}$$

$$\Delta p = (\Delta P)_{aerodynamic} + (\Delta P)_{internal} + \frac{(\rho_a - \rho_{he})gd}{2} \tag{8}$$

Where

$$(\Delta P)_{aerodynamic} = 1/2\rho_a V^2 C_p \tag{9}$$

$$(\Delta P)_{internal} = 1.15 * (1/2\rho_a V^2) \tag{10}$$

VII. SIMANN Optimizer

The SIMANN SA code developed by Goffe et al.[8] based on the methodology proposed by Corana et al[9] for objective functions involving continuous variables was employed for optimization. The algorithm starts with a high initial value of annealing temperature T_{init} and a starting set of design variables. Trial sets are then generated using random numbers from the set [-1,1] and initial step length for each design variable v_i. If the function value for the trial set is lower than that for the previous one, the trial set is accepted. Acceptance of a trial set yielding higher function value is random, with a probability decreasing exponentially with the temperature. After N_S steps through all design variables, their step lengths are adjusted, to ensure that roughly half of all the moves are accepted using a varying criterion c_i, in line with the approach followed by Metropolis et al.[10] A very high acceptance rate implies that the function domain is not being fully explored,while a very low acceptance rate means that the new trial points are being generated too far away from the current optimum. Both of these imply that the algorithm is not progressing efficiently and involves wasting of computational effort. After carrying the above loop N_T times, the annealing temperature is gradually reduced employing a geometric schedule governed by the parameter r_t. The algorithm is stopped when the reduction in the function value in N_{eps} successive cycles is less than a small number *eps*. As with all general purpose optimization methods, some control parameters in SIMANN had to be "tuned" to suit the objective function, and to ensure that the optimizer performs efficiently. A bad choice for these parameters can make the algorithm extremely inefficient and may even result in failure to arrive at the global optimum. The eight such parameters in SIMANN are T_{init} , v_i , N_S, c_i , N_T, r_t, N_{eps} and *eps*. Values of 1.0, 20, 30, 0.85,2.0, 2 are assigned for v_i , N_S, c_i , N_T, r_t, N_{eps} respectively, as recommended by Corana et al,[9] and based on previous experience. The most suitable values of the remaining 3 parameters viz. T_{init} , are determined by numerical experimentation. A higher penalty is forced on the objective function for the undesired shapes resulted through the shape generation algorithm.

VIII. Results and Discussion

A. C_{DV} as Objective Function

The optimized shape resulted for C_{DV} as objective function is compared with GNVR shape as shown in figure 8. Table 1 shows the comparison of various parameters for optimized and GNVR shape. The marginal improvement of 1.3% is observed in drag or C_{DV} with low fidelity analysis. The shape offers marginal improvement in surface area with higher penalty on stress. The thickness ratio for the optimized shape is greater than that of GNVR shape resulting in lesser drag as seen from Eq.6.

B. Verification using *Fluent* Results

It is needed to estimate the actual C_{DV} with high fidelity analysis to verify the practical applicability of the results obtained using the low fidelity model. The shape resulted from optimizer for minimum C_{DV} is tested using CFD code *Fluent* with the similar grid and boundary conditions as that of GNVR shape. The comparison for optimized body with GNVR shape for low and high fidelity analysis is presented in table 2 . It can be seen that the drag for optimized shape is 27% greater than GNVR hull shape as obtained using high fidelity model which is in complete contrast to the results predicted by low fidelity model.

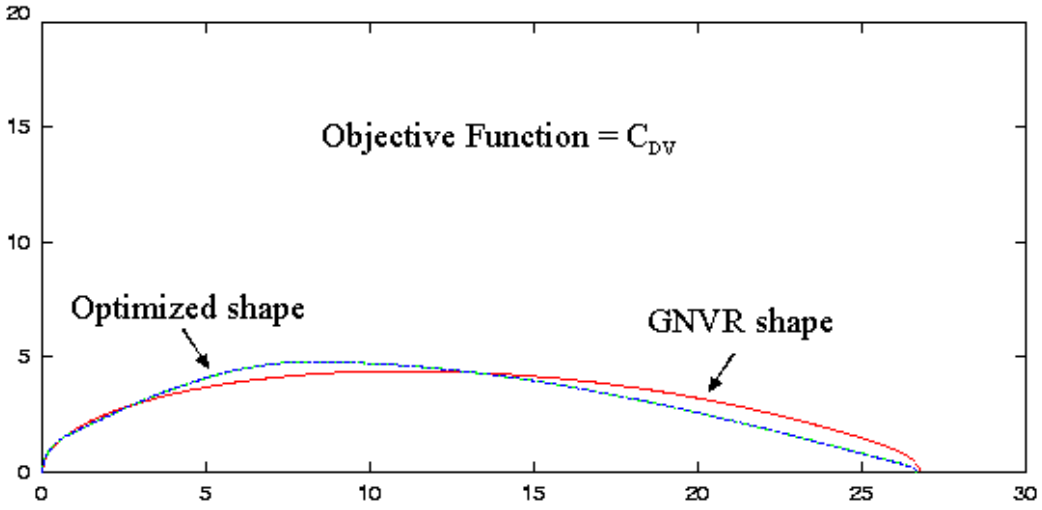

Figure 8. Comparison showing Optimized Shape for C_{DV} and GNVR shape

Table 1. Comparison of Optimized Shape for C_{DV} and GNVR Shape using Low Fidelity

	GNVR Shape	Optimized Shape	% Improvement
Thickness Ratio (d / l)	0.160	0.178	-
C_{DV} (Obj. Function)	1.6902E-02	1.6678E-02	1.3%
Surface Area (m^2)	573.1	560	2.3 %
σ_{max} (N/m)	4457	4924	-10.5 %

Table 2. Comparison between the Results Predicted by Low Fidelity and *Fluent* code

Model	GNVR Shape	Optimized Shape	% Improvement
C_{DV} Low Fidelity	1.6902E-02	1.6689E-02	1.3 %
C_{DV} *Fluent* Code	2.622E-02	3.338E-02	-27.0 %

IX. Intermediate Fidelity Model for C_{DV}

The results presented in table 2 prompts to improve the low fidelity model for estimating C_{DV} . The large variation in predicted value of C_{DV} is considered due to the pressure drag. Lutz *et.al*[11] has reported that the total drag for airship like bodies is a function of position of maximum diameter and surface area. The position of maximum diameter along the length of the hull decides the pressure drag whereas the surface area mainly contribute to skin friction drag. This fact helps to understand that for a body having fixed

thickness ratio (d/l), total drag can vary appreciably if either the position of maximum diameter or surface area changes.

The variation of C_{DV} with surface area was studied using the data obtained through the *Fluent* code for the bodies having same thickness ratio as that of GNVR shape. It was observed that for 4.5% change in surface area, C_{DV} vvalue changes by 2.5%. Similar study was made to see the effect of position of maximum diameter on volumetric coefficient of drag C_{DV} . Figure IX shows the variation of C_{DV} with respect to (X_{ymax}/l). It is seen from the graph that as (X_{ymax}/l) value increases C_{DV} ddecreases as a consequence of reduced pressure drag. 80% variation in (X_{ymax}/l) causes C_{DV} to vary by 42%. So the sensitivity of C_{DV} with respect to surface area and (X_{ymax}/l) is nearly the same.

Though for the same thickness ratio surface area and $(X_{ymax}/\mathrm{l}\ )$ seem to affect C_{DV} vvalue equally, it can be argued that with the increase in maximum diameter for same length will induce more pressure drag as the projected area increases in proportion to d^2. Moreover the absolute variation in C_{DV} for the shape configuration with constant (d/l) considered is very high (80%) for the change in the parameter (X_{ymax}/l). Since the original expression for C_{DV} is not very much able to take the effect of pressure drag, current low fidelity model for C_{DV} is updated using C_{DV} vvariation with (X_{ymax}/l). To retain the feature of original equation, the difference between C_{DV} oobtained using *Fluent* code and that using original low fidelity analysis is considered for curve fitting.A third degree polynomial is fitted by the least square method. The new expression arrived for C_{DV} is presented in the form of Eqn.11 where C_{DV} is calculated using Eqn.6

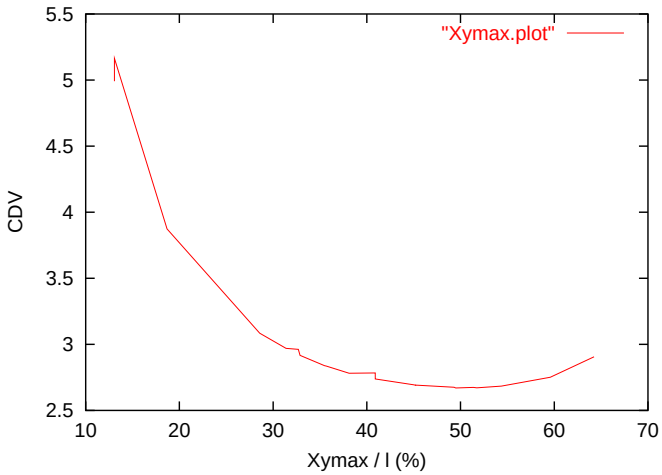

Figure 9. C_{DV} **Vs** $(X_{ymax}\%/l)$ **for Fixed Thickness Ratio**

$$C_{DV\,mod} = C_{DV} + (-37.54\overline{X}^3 + 61.55\overline{X}^2 - 32.568\overline{X} + 6.6033)E - 02 \tag{11}$$

Where $\overline{X} = (X_{ymax}/l)$

X. Results with Intermediate Fidelity

The optimizer is incorporated with improved C_{DV} mmodel given by Eq. 11 and result is obtained for C_{DV} as objective function. Figure 10 compares the resulted shape with GNVR shape. It can be seen that the configuration for optimized envelope shape is appreciably closer to GNVR shape. Comparison in terms of numerical values for various objective function is shown in table 3.

A. Verification using *Fluent* Code

Table 4 compares the results using intermediate fidelity to that obtained using *Fluent* code. The intermediate fidelity analysis gives the idea of aerodynamically better shape than GNVR as seen in table 3, whereas the same is contradicted by the high fidelity results showing increase in the drag by 11.5% for optimized body as compared to GNVR body. Referring to table 2 again, it can inferred that the results using intermediate fidelity are better than low fidelity since the actual drag for the optimized body resulted using former is 12.5%

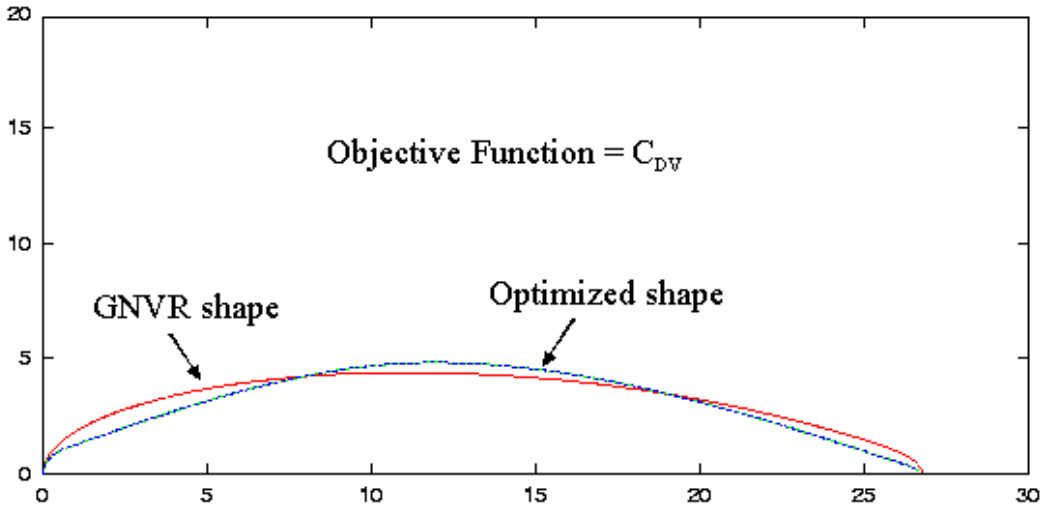

Figure 10. Optimized Shape with Improved Fidelity Model for C_{DV} Vs GNVR Shape

Table 3. Results with Improved Fidelity

	GNVR Shape	Optimized Shape	% Improvement
Thickness Ratio (d / l)	0.16	0.1807	
C_{DV} (Obj. Function) Intermediate Fidelity	2.702E-02	2.6619E-02	1.5%
Surface Area (m^2)	573.1	557.4	2.7%
σ_{max} (N/m)	4457	4903	-10.0 %

less than that predicted with latter. To model the physics more accurately sufficiently large experimental data is required to be obtained for the bodies with varying thickness ratios.

Table 4. Comparison Showing the Results Predicted by Intermediate Model and *Fluent* Code

Model	GNVR Shape	Optimized Shape	% Improvement
C_{DV} Intermediate Fidelity	2.702E-02	2.6619E-02	1.5 %
C_{DV} *Fluent* Code	2.622E-02	2.922E-02	-11.5 %

B. Result for Variable Length Configuration

The length of the envelope so far was constrained to remain fixed. To explore the possibility of other aerodynamically better shape, the fixed length constraint is relaxed and length is allowed to vary between 25.0 - 30.0 m. The optimized shape for C_{DV} is compared with that resulted for fixed length and is shown in figure 11. It is interesting to note that the optimized shape with fixed length and variable length configuration matches closely to each other. Thus minimum drag shape has the same length as that of GNVR shape with the condition of fixed volume as the main constraint.

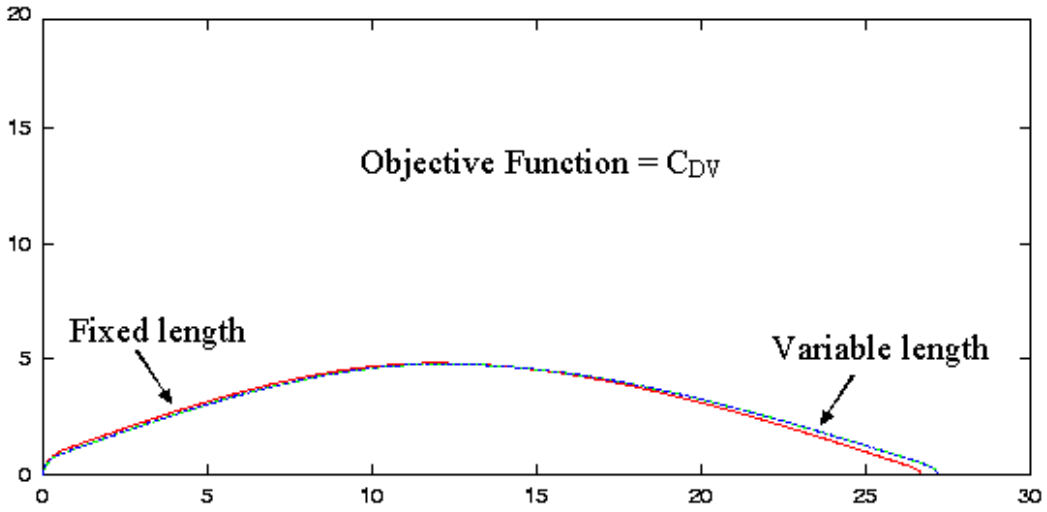

Figure 11. Optimized Shapes for C_{DV} with Fixed and Variable Length Configurations

XI. Further Improvement in the C_{DV} Model

The intermediate fidelity model is found to be inadequate when applied to the shapes with thickness ratios different from GNVR shape. The main idea of further improving the intermediate fidelity model for C_{DV} is to closely examine the various feasible shapes spread across the entire design space and determining the dominant geometric parameters which directly influence the aerodynamic characteristics of an envelope. In the present study, similar approach is adopted where sufficient number of experiments were conducted using *Fluent* code for family of shapes corresponding to one thickness ratio.The length was allowed to vary between $25m$ to $30m$. The shapes were found to lie between the thickness ratio 0.14 to 0.21. The detail study of these shapes has resulted in three geometric parameters other than X_{ymax} to predict C_{DV} for the given envelope shape. The concerned geometric parameters has been named as α_1, α_2, α_3 and are described below

$$\alpha_1 = \frac{d}{l - X_{ymax}}$$

$$\alpha_2 = \frac{\sum_{x=0.9l}^{l} (dy/dx)}{l.N}$$

$$\alpha_3 = \frac{\sum_{x=0}^{0.1l} (dy/dx)}{l.N}$$

These three parameters and X_{ymax} are combined together to arrive at a single geometric parameter 'α' given as

$$\alpha = \alpha_1.\alpha_2^{\beta}.\alpha_3.X_{ymax} \tag{12}$$

The slope (dy/dx) for the concerned shape configuration at $x = 0$ and $x = l$ is thereotically infinite and is taken care numerically by omitting the point on leading and trailing edge in the calculations of the parameters α_2 and α_3. The actual computation of the slopes starts at a distance of the order of 0.05 away from both the edges. N indicates the number of grid points considered across the initial 10% length for α_1 estimation and trailing 90% length for α_2 estimation. The parameter β is calculated as a function of thickness ratio.

It becomes clear from the observed variation of β with (d/l) shown in figure 12, that the curve follows the linear nature from (d/l) - 0.16 onwards and is essentially invariant below this threshold. The second or higher degree fit for β to account for all the points would result in appreciably higher error particularly for the shapes with lower thickness ratios in this case. In the present approach the β has been estimated conditionally as

$$\beta = \begin{cases} 214.(d/l) - 31.26 & \beta > 3 \\ 3 & \text{Otherwise} \end{cases} \tag{13}$$

The conditional estimation along with the linear fit depicted in Eqn.13 improves the accuracy by inducing the lower order errors in the curve fit model.

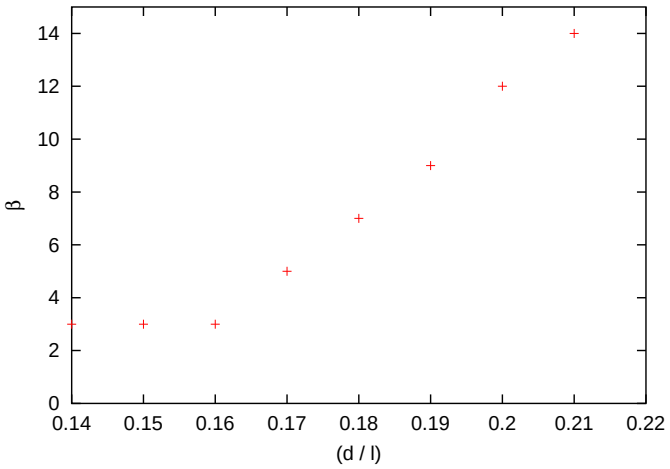

Figure 12. Variation of β with (d/l)

The coefficient of drag based on surface area C_D has been used in the model rather than C_{DV} as a consequence of smoother variation of C_D with α. Figure 13 shows the variation of C_D with α for various thickness ratio. Similar graphs have been resulted for rest of the thickness ratios. The linear fit for these graphs has resulted in R^2 value between (0.95-0.997) showing a maximum error of 4.5% in the design space considered.

$$C_D = (A.\alpha + B)E - 04 \tag{14}$$

The coefficients A and B are again obtained as the functions of thickness ratio. Figure 14 shows the variation of A and B with thickness ratio respectively. The similar approach as that for variable β has been adopted for conditional estimation of coefficient 'A' and is given by Eq.15. The coefficient 'B' is estimated using linear equation given in the form of Eq.16 as also obvious from figure 14.

$$A = \begin{cases} -12.02.(d/l) + 2.068 & A > 0 \\ 0 & \text{Otherwise} \end{cases} \tag{15}$$

$$B = 342.9.(d/l) - 13.50 \tag{16}$$

The required objective function C_{DV} can readily be estimated from C_D using Eq.1

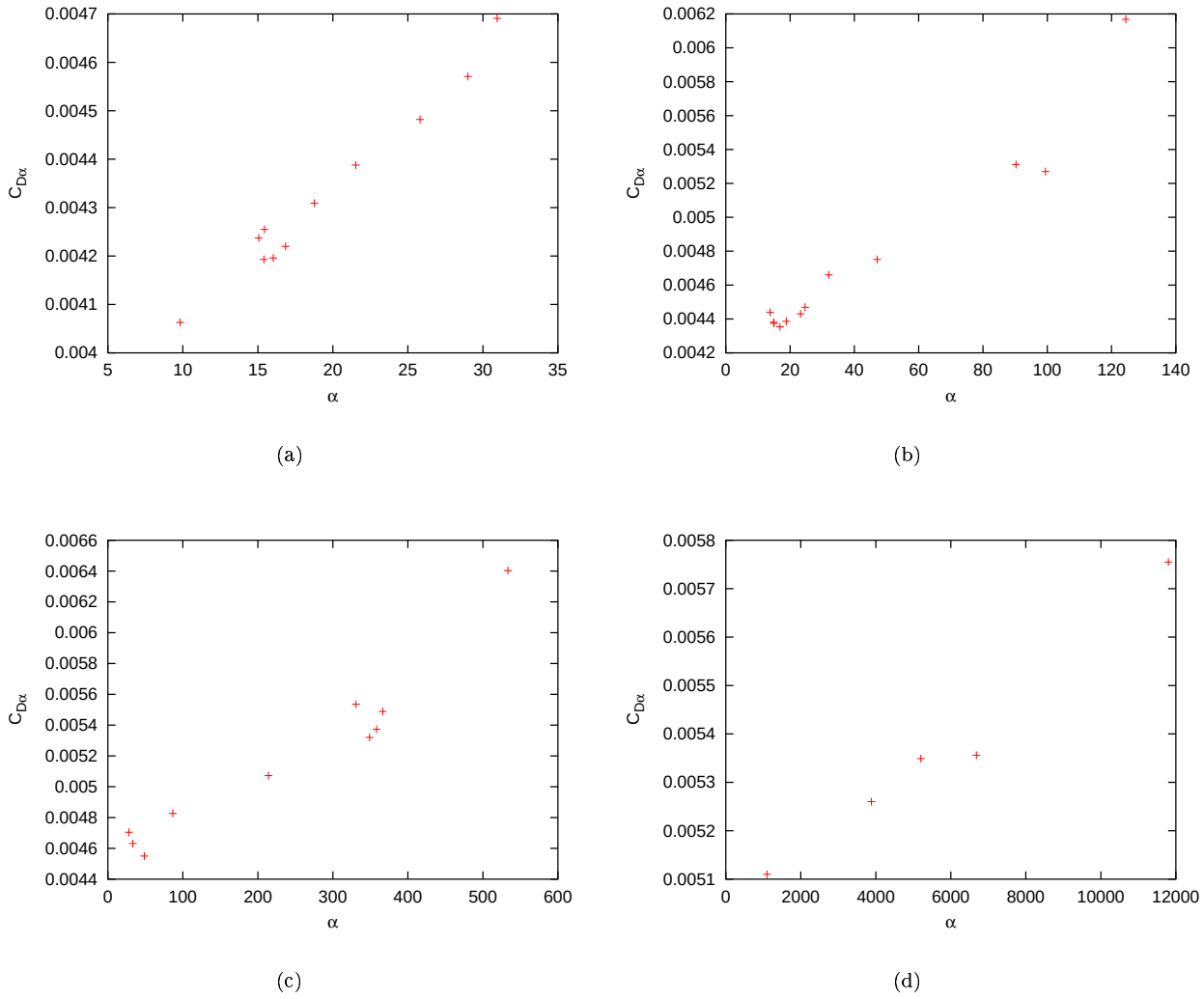

Figure 13. Variation of $(C_D)_\alpha$ with α

A. Validation of Improved Fidelity

Among the various feasible shapes which were excluded during the experimentation with *Fluent* code, some of the shapes are used to validate the improved fidelity model. The shapes are predominantly distinguished by the parameter X_{ymax} . Table 5 shows the comparison between predicted value of C_D by improved fidelity and that obtained using *Fluent* code. It can be observed that absolute percentage error is high for shapes with higher thickness ratios and is well within 5%. The linear nature of Eq. 14 confirms the numerical errors of lower order in the estimated C_D value.

XII. Results with Improved Fidelity

The improved fidelity model is integrated with the SIMANN optimizer and results were obtained for the cases of fixed length and variable envelope length configurations with C_{DV} and surface area as the objective

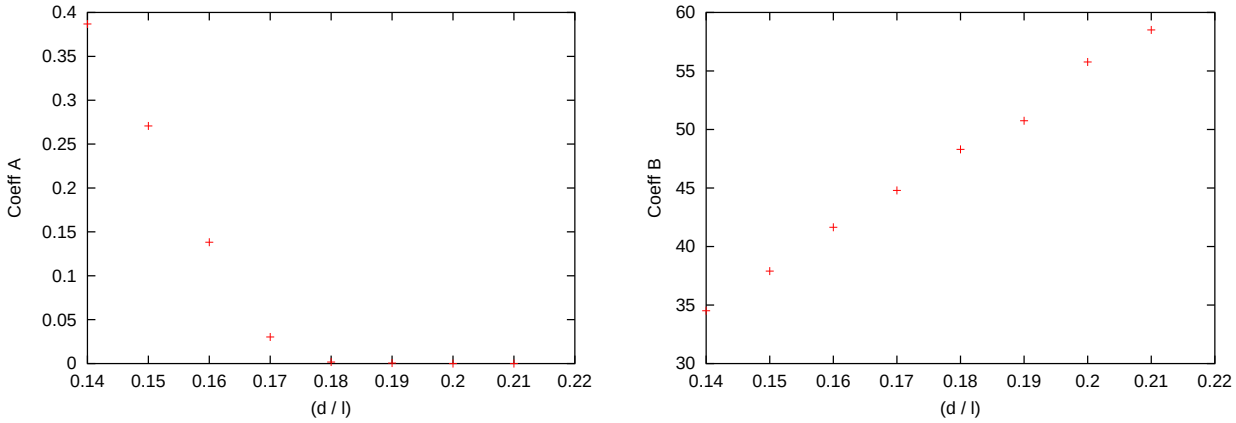

(a) Variation of Coeff. 'A' with (d/l)

(b) Variation of Coeff. 'B' with (d/l)

Figure 14. Variation of Coefficient A and B with (d/l)

Table 5. Comparison Showing the Results Predicted by Improved Fidelity and *Fluent* Code

Shape No.	(d/l)	X_{ymax}	**Improved Fidelity** C_D	***Fluent* code** C_D	**% Error**
1	0.142	13.6	2.317E-02	2.357E-02	1.7%
2	0.140	10.55	2.343E-02	2.436E-02	3.8%
3	0.151	10.05	2.595E-02	2.655E-03	2.2%
4	0.155	15.65	2.585E-02	2.606E-02	0.8%
5	0.146	17.00	2.497E-02	2.485E-02	0.5%
6	0.163	16.55	3.018E-02	3.018E-02	0.0%
7	0.164	16.0	2.723E-02	2.669E-02	2.0%
8	0.172	15.8	2.893E-02	2.865E-02	1.0%
9	0.175	8.85	3.012E-02	3.097E-02	2.5%
10	0.185	8.85	3.055E-02	2.958E-02	3.3%
11	0.183	10.0	3.057E-02	2.977E-02	2.7%
12	0.190	12.8	3.264E-02	3.151E-02	3.6%
13	0.196	9.0	3.438E-02	3.290E-02	4.5%
14	0.197	12.9	3.166E-02	3.082E-02	2.7%

function.

A. C_{DV} as Objective Function

In the first case the length is constrained to have the same length as GNVR shape i.e. 26.77 m with 0.5% tolerance on either side to avoid the numerical discrepancies. In the later case the length is allowed to vary

between $(25 - 30)m$. Figure 15 shows the resulted shapes in comparison with GNVR shape. Table 6 compares the resulted shapes for both the cases with GNVR shape in terms of relevant objective functions. Optimized shape for fixed length configuration shows little improvement in C_{DV} and surface area with lower penalty on σ_{max} . The results with variable length configuration are remarkable showing around 16% improvement in C_{DV} with smaller variation in the surface area and σ_{max} vvalue.

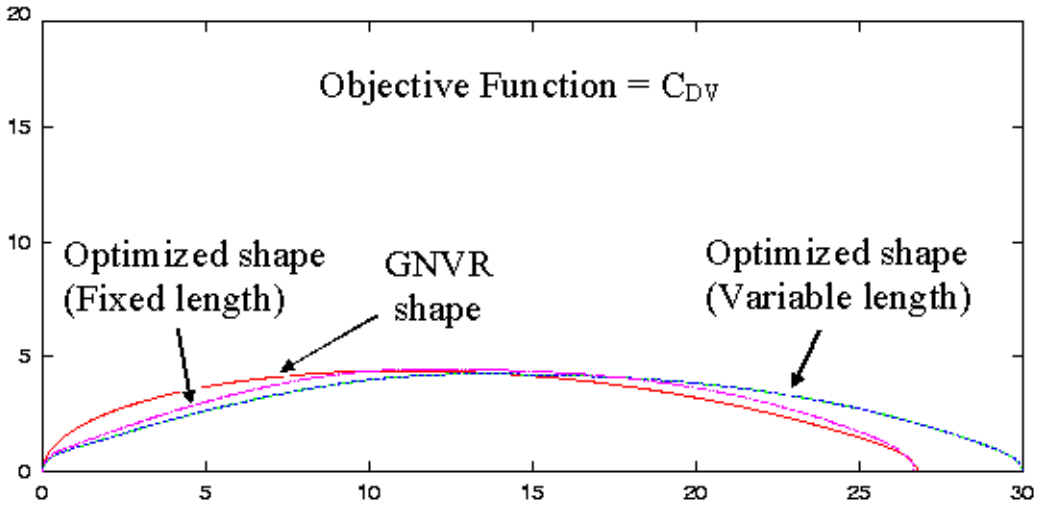

Figure 15. Comparison Showing Optimized Shapes for Fixed and Variable Length Configurations Vs GNVR Shape

Table 6. Results with Improved Fidelity

	GNVR shape	**Optimized shape (Fixed length)**	**Improvement (%)**	**Optimized shape (Variable length)**	**Improvemen (%)**
Thickness Ratio (d / l)	0.16	0.1669	-	0.1415	-
C_{DV} (Obj. Function) Improved Fidelity	2.686E-02	2.665E-02	0.8%	2.233E-02	16.3%
Surface Area (m^2)	573.1	568.3	0.8%	593.6	-3.6%
σ_{max} (N/m)	4457	4525	-1.5 %	4309	3.3%

Verification using Fluent Code

Table 7 compares the C_{DV} vvalues predicted using improved fidelity model with *Fluent* code. The C_{DV} vvalue for fixed length configuration is observed to be appreciably close to *Fluent* code value showing a slight improvement in C_{DV} . On the conrary *Fluent* code predicts little higher drag than GNVR shape for optimized shape. The improvement over GNVR shape given by improved fidelity and *Fluent* code is small and hence can be attributed to the numerical error arising out of computations and approximation through

Table 7. Comparison Showing the Results Predicted by Improved and *Fluent* code

Model	GNVR shape	Optimized shape (Fixed length)	Improvement (%)	Optimized shape (Variable length)	Improvement (%)
C_{DV} Improved Fidelity	2.686E-02	2.665E-02	0.8 %	2.233E-02	16.3%
C_{DV} *Fluent* code	2.622E-02	2.655E-02	-1.3 %	2.310E-02	11.8%

curve fitting. This fact can be made use of to infer that the resulted shape is the optimized shape for the fixed length configuration. This can be further backed by observing figure 7 that the exact GNVR shape is not possible with shape configuration considered for the present study.

C_{DV} vvalue predicted using improved fidelity for variable length configuration differs by 3.5 % to that resulted using *Fluent* code as seen in Table 7. The shape shows significant improvement in the drag of around 16% as predicted by the improved fidelity where the actual improvement was observed to be around 12% using *Fluent* code. This proves at first hand, the superiority of the currently developed model compared to earlier two models discussed in this paper.

B. Surface Area as Objective Function

The similar experiment is carried out with surface area as objective function for the cases of fixed length and variable length. The shapes obtained for both the cases are compared to the GNVR shape and is depicted in figure **??**. From the comparison shown in figure 16, it can be inferred that the configuration prefers to have minimum length for minimum surface area. Table 8 shows the comparison with respect to all the objective functions.

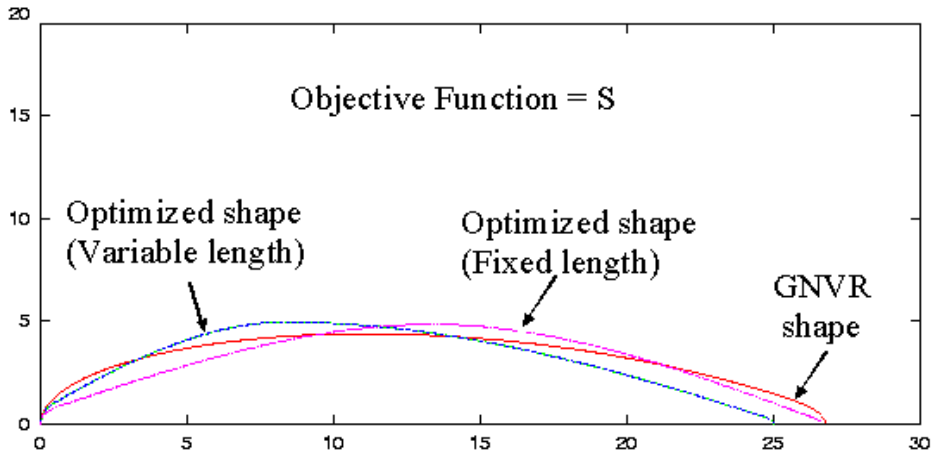

Figure 16. Optimized Shapes for 'S' with Fixed and Variable Length Configurations Vs GNVR Shape

Table 8. Comparison for Min.'S' Shapes for Fixed and Variable Length Configurations

	GNVR shape	Optimized shape (Fixed Length)	% Imprvmt over GNVR	Optimized shape (Variable Length)	% Imprmnt over GNVR
(d / l)	0.16	0.1821		0.1981	
C_{DV}	2.686E-02	2.718E-02	-1.2%	3.620E-02	-21.4%
S (m^2) (Objective Fucn.)	573.1	555.1	3.2%	545.9	4.7%
σ_{max} (N/m)	4457	4931	-10.6%	5042	-13.12%

XIII. Multi-Disciplinary Optimization using Composite Objective Function

The cases studied so far were pertaining to single objective function. To appreciate the multi-disciplinary aspect of optimization a composite objective functions comprising of C_{DV} 'S' and σ_{max} has been devised where the indivisual objective function has been normalized using the respective values corresponding to GNVR shape. The objective function is represented as follows

$$F_{comp} = w_1.[\frac{C_{DV}}{(C_{DV})_{GNVR}}] + w_2.[\frac{S}{(S)_{GNVR}}] + w_3.[\frac{\sigma_{max}}{(\sigma_{max})_{GNVR}}] \quad (17)$$

Where w_1,w_2 and w_3 are weight functions. For the present case all the weight functions have been assigned a value unity. Figure 17 shows the optimal shape and GNVR shape. The numerical values of three objective functions are presented and compared to GNVR shape in Table 9.

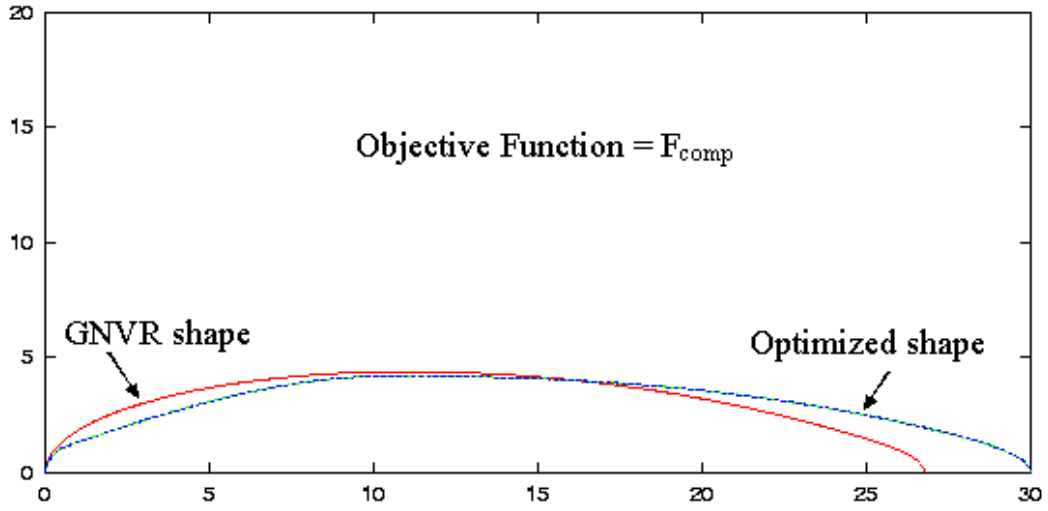

Figure 17. Comparison Showing Optimized Shape with Composite Obj. Function Vs GNVR Shape

The actual C_{DV} vvalue predicted by *Fluent* code is found to be close to that predicted using improved fidelity model proving the reliability of the result presented in table 9 to an appreciable extent. The resulted

Table 9. Multi-Disciplinary Optimization using Composite Objective Function

	GNVR Shape	Optimized Shape	% Improvement
(d/l)	0.160	0.140	-
C_{DV}	2.686E-02	2.260E-02	15.8 %
'S'(m^2)	573.1	598.7	-4.5%
σ_{max} (N/m)	4457	4262	4.4 %
F_{comp}	3.0	2.8	6.7%

shape can be considered as the optimized shape for the constraint of fixed volume and manufacturability avoiding convex shapes directly in the shape generation algorithm.

XIV. Conclusion

The coefficient of pressure C_p distribution around a reference GNVR shape obtained using *Fluent* code found to be matching to that arrived using source panel method except near the trailing edge due to flow seperation. This fact has been used to validate *Fluent* code for the current application. The slapping technique for CFD solution used, found to give the convergence much faster saving up to 40% of computational time per geometry. The initial strategy involves the parameterization using of the geometry with basic shapes using two dimensional design vector. Optimization technique using DACE ,being economical for small design vector has been implemented and it is observed that the resulted shape closely matches to the GNVR shape. The C_{DV} as a function of (d/l) as suggested in the literature found to give the results largely varying from the actual. The present study has indicated that, C_{DV} is a function of X_{ymax} and surface area other than thickness ratio.

The parameter X_{ymax} , has been used to improve the C_{DV} model to arrive at the intermediate fidelity level. It was observed that the results obtained are in contradiction to that given by *Fluent* code. Sufficiently large number of experiments were conducted to further improve the model for C_{DV} . The geometric parameters which directly influences the aerodynamic characteristics of the shape have been analyzed and inducted in the C_{DV} model. The improved model is in the form of linear fit for C_{DV} where the coefficients and power were obtained as a function of thickness ratio. The validation using some of the feasible test points shows the absolute error well within 5.0%.

The resulted shape for variable length configuration observed to offer lesser drag than GNVR shape showing a remarkable improvement of 11.8% in C_{DV} . The resulted value of C_{DV} for the cases of fixed length and variable length configuration found to be closely matching to that given by *Fluent* code. The results were obtained for surface area as objective function for fixed length and variable length configuration and it was observed that the variable length configuration achieves the minimum length allowed, for minimum surface area. To address the multi-disciplinary nature of the problem a composite function has been devised comprising of normalized values of C_{DV} S,and σ_{max} with respective weightages. The indivisual objective functions has been normalilzed with respect to the respective GNVR parameteres. It was observed that the composite objective function value comes out to be lesser than GNVR shape.

References

[1]Hoerner S.F.,*Fluid-Dynamic Drag* Midland Park, N.J., 1965

[2]Gillett J.D., "Airship Technology", Cambridge Aerospace Series, 1999, pp. 181.

[3]Narayana C.L., and Srilatha K.R., "Analysis of Aerostata Configuraton By Panel Method," PD CF 0010, July 2000, NAL, Bangalore.

[4]Z. Pateka and L. Smrcek,."Aerodynamic characteristics of multi-surface aircraft configurations", *Aircraft Design*,Volume 2, December 1999, pp.191-206

[5]Rachid Younsi, Ismail El-Batanony, Jeur-Bernard Tritsch, Hassan Naji and Bernard Landjeri.,"Dynamic study of a Wind Turbine Blade with Horizontal Axis", *European Journal of Mechanics - A/Solids*,Volume 20, March 2001, pp. 241-252

[6]Jones S. P. and DeLaurier J.D.,"Aerodynamic Estimation Techniques for Aerostats and Aeroships" ,*Journal of Aircraft*, Vol 20, Feb. 1983, pp.120-126.

[7]Pant, R., Gawale, A., "Design, Fabrication And Flight Testing Of Remotely Controlled Airship",*National Conference on LTA Technologies*, Aerial Delivery R&D Establishment, Agra,India, October 2002, pp.4-6

[8]Goffe, W. L., G. D. Ferrier, J. Rogers. (1994). Global Optimization of Statistical Functions with Simulated Annealing, Journal of Econometrics, 60, 65-100.

[9]Corana, A., Marchesi, M., Martini, C. M. and Ridella, S. (1987) Minimizing multimodal functions of continuous variables with the Simulated Annealing algorithm. ACM Transactions on Mathematical Software, 13, 262-280.

[10]Metropolis, N., Rosenbluth, A., Rosenbluth, M., Teller, A. and Teller, E. (1953) Equation of state calculations by fast computing machines. Journal of Chemical Physics, 21, pp. 1087-1090.

[11]Th.Lutz,Schweyher H.,Wagner S.,"Shape Optimization of Axisymmetrc Bodies in Incompressible Flow" , *Journal of Aircraft*, Vol 20, Feb. 1985, pp.520-526